Powder Metallurgy and Metal Ceramics, Vol. 53, Nos. 1-2, May, 2014 (Russian Original Vol. 53, Nos. 1-2, Jan.-Feb., 2014)

NANOSTRUCTURED MATERIALS

NANOCOMPOSITES BASED ON REFRACTORY COMPOUNDS, CONSOLIDATED BY RATE-CONTROLLED AND SPARK-PLASMA SINTERING (REVIEW)

O. B. Zgalat-Lozinskii[1]

UDC 621.762.52/621.762.53

Rate-controlled sintering and spark plasma sintering are considered the most promising methods to produce dense nanoctructured ceramics. Refractory compounds are used to demonstrate the application of methods for controlling the densification rate and nonlinear heating and loading conditions to produce dense nanocomposites with 30–70 nm grains. The mechanical and tribological properties of ceramics with grains from 50 to 500 nm in size are compared. The effect of increase in the mechanical (5–15%) and tribological (to 50%) characteristics of nanocomposites consolidated by rate-controlled sintering and modified nonlinear spark plasma sintering is studied. Nanocomposites based on refractory nitrides and borides are regarded as promising materials for creating a new generation of cutting tools, as well as wear-resistant ceramics for wide application.

Keywords*: TiN, TiCN, Si_3N_4, nanocomposites, sintering, spark plasma sintering, shrinkage.*

INTRODUCTION

A number of theoretical studies [1–4] on modelling the variation of material properties with the dimensions of its structural elements show that decreasing grain size to 100 nm or less (nanoscale) causes the material to demonstrate extreme properties (hardness, strength, wear resistance, etc.). For example, the classical Petch–Hall equation suggests that the strength (hardness) of material linearly increases with decreasing grain size, which was the basis for finding extremely hard (strong) nanomaterials. However, no substantial progress has been made toward achieving the maximum mechanical characteristics of ceramic solids by decreasing the grain size. Only the hardness of thin films based on refractory compounds can be made comparable with that of diamond by decreasing the grain size [3]. A structural analysis of nanomaterials shows that decreasing the grain size to tens of nanometers increases the volume of grain boundaries and, hence, their contribution to the properties of the material. To assess the effect of grain boundaries on the hardness of the material the following modified Petch–Hall equation is proposed in [1]:

$$H = H_g \cdot (1 - f) + H_{gb} \cdot f, \tag{1}$$

where H_g is the hardness of grains, H_{gb} is the hardness of grain boundaries, f is the volume of grain boundaries.

[1]Frantsevich Institute for Problems of Materials Science, National Academy of Sciences of Ukraine, Kiev, Ukraine; e-mail: ostap@ipms.kiev.ua.

Translated from Poroshkovaya Metallurgiya, Vol. 53, No. 1–2 (489), pp. 26–40, 2014. Original article submitted May 16, 2013.

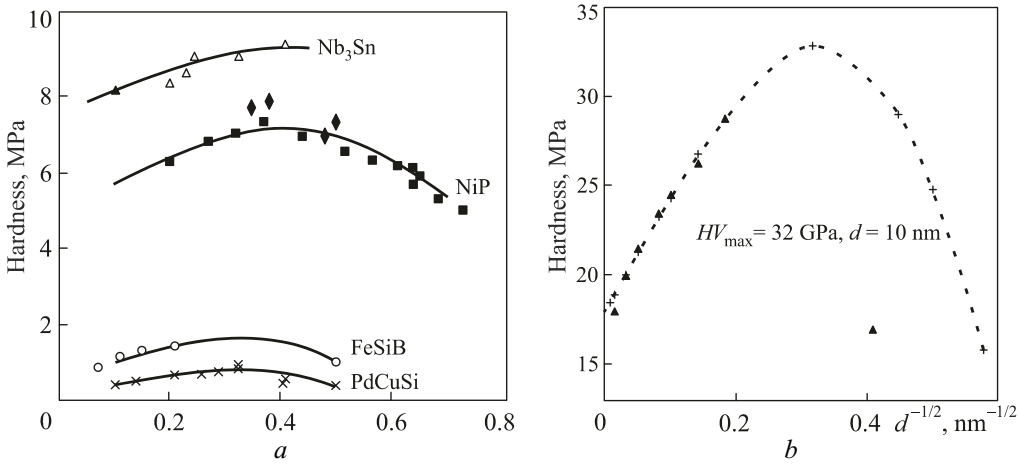

Fig. 1. Variation of hardness with the grain size of nanomaterials (*a*) [1] and titanium nitride (*b*) [5]

The above theory is in good agreement with practical results (Fig. 1), is supplemented by the data from [4] to understand the "softening" effect, and can be used to calculate the critical grain size at maximum hardness.

Following the new approaches [1] to evaluate the hardness of nanomaterials, a prediction was made in [5] to achieve the maximum hardness of titanium nitride depending on the grain size. The experimental and calculated values of hardness were also compared. Titanium nitride was chosen as a basis for the material (see the literature for its properties). Also, it is a component of many composites widely used in the industry [2, 6, 7].

The prediction [1] was made using Eq. (2) that allows for the contribution of hardness of both grains and grain boundaries to the total hardness of the material:

$$H = H_{\mathrm{g}} + k_{\mathrm{af}} \cdot \left[\frac{(d-\delta)^3}{d^3} + \frac{d^3 - (d-\delta)^3}{d^3} \cdot \left(\frac{\ln \dfrac{\vartheta \cdot d}{r_0}}{\ln \dfrac{\vartheta \cdot d_c}{r_0}} \right) \right] \cdot d^{-1/2}, \tag{2}$$

where k_{af} is an adjusting factor; d is the grain diameter; δ is the thickness of grain boundary; ϑ is a numerical factor less than 1; d_{c} is the critical grain size for dislocation movement; r_0 is the radius of dislocation core.

The maximum hardness of titanium nitride can make ~32 GPa at a grain size of ~10 nm (Fig. 1*b*), which agrees with the calculated value for dislocation movement in titanium nitride [5].

However, a number of important problems should be resolved to fully understand the anomalous behavior of nanocrystalline systems:

- production of dense nanostructural ceramics with minimum content of impurities;
- study of grain boundaries in nanocrystalline materials and dislocations at critical grain size;
- analysis of the results to identify the mechanisms of abnormal hardness and "softening" of materials with superfine structure;
- production of nanostructural ceramics with volume >1 cm^3 and uniform distribution of structural elements over it.

Our goal here is to examine the possibilities for the formation of nanostructural ceramics by rate-controlled sintering (RCS) and spark plasma sintering (SPS), which allow producing a dense refractory ceramics with grains smaller than 100 nm. The consolidation process is optimized by shrinkage control and the technological cycle for manufacturing products of various shapes can be scaled to commercial production.

RATE-CONTROLLED SINTERING

The RCS technique was used as a structural-oriented type of sintering that substantially limited the grain growth compared to conventional pressureless sintering and produced dense ceramics with high hardness, fracture-

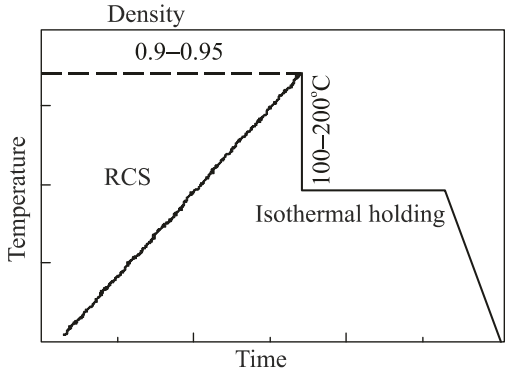

Fig. 2. Modified RCS of nanopowders

resistance, and strength [8, 9]. The main advantage of the RCS technique over conventional pressureless sintering is that it is possible to achieve a final density of ~99.9% of theoretical density keeping the grain size less than 100 nm.

The RCS technique is described in [10–14] where the multi-stage rate–density profile depending on the nature of the material and the powder particle size is considered to be unique. The basic task of RCS is to determine the maximum densification rate and, thus, to select the optimal sintering mode by analyzing dilatometric tests on sintering with constant heating rates. Varying the heating rate, it is possible to obtain data on the behavior of the material under nonisothermal conditions. The data are used to plot a kinetic field of response (KFR), i.e., the projection of the response surface $D–d/dt–T$ onto the plane of Arrhenius coordinates $\ln(T \cdot d/dt)$ and $10^4/T$, and then the temperature–time profile. One KFR may be used to plot several profiles that meet the RCS requirements. In this case, the optimality criterion could be the grain size or any other material characteristic.

In addition to RCS, a technique for abrupt reduction in sintering temperature at the final stage [16] to additionally suppress grain growth during the consolidation of nanocrystalline materials was proposed in [15]. RCS underlies the modified sintering technique: the temperature drop point and isothermal holding temperature are taken from the RCS-profile, which is plotted using a KFR. RCS allows forming a homogeneous porous structure in the material until reaching a density of up to 90–95% of the theoretical density. After that, with decrease in temperature and holding time, the homogeneous porous structure also uniformly evolves to 100% density.

Figure 2 schematizes the consolidation of nanostructured powders. In the first stage, the RCS mode calculated from the KFR was used until the material density reached 0.9–0.95 of the theoretical density. The second stage involved an abrupt reduction in sintering temperature by 100–200°C and isothermal holding for 5–15 min at set temperature [5, 15–17].

RCS of TiN Nanopowder. To study the proposed sintering mode (Fig. 2), the optimal consolidation parameters of TiN nanopowder were determined [15, 17]. The sintering mode was optimized with respect to maximum allowed heating rate, porosity and grain size of nonisothermally sintered ceramics. Based on the data obtained, a few RCS modes were tested and the holding time that allows achieving the optimal TiN grain size–porosity ratio was chosen. An analysis of porosity–grain size–temperature relationship revealed that after the temperature reached the threshold 1200–1300°C, not only the volume of structural defects substantially decreased, but also in-plane porosity dropped to zero and defect-free grain boundaries formed in the sintered material [15, 17]. A temperature of ~ 1300°C is critical for TiN nanopowder sintering. At temperatures higher than 1300°C, grains show an uncontrolled growth to over 100 nm. Therefore, to retain a nanostructural state during the consolidation of 15–50 nm TiN nanopowders, the heating stage must be completed before 1300°C. The residual porosity of sintered ceramics may exceed 5% at 1250–1300°C.

To consolidate nano-TiN, a multistage RCS mode with decrease in temperature and holding for several minutes (Fig. 3) was applied in [15]. This made it possible to decrease the sintering temperature to 1150–1250°C and to reach a residual porosity of less than 1.5%. The TiN samples sintered in vacuum using the modified RCS mode had a fine structure (50–70 nm), “clean” grain boundaries (Fig. 4), and demonstrated a nanohardness of ~26 GPa.

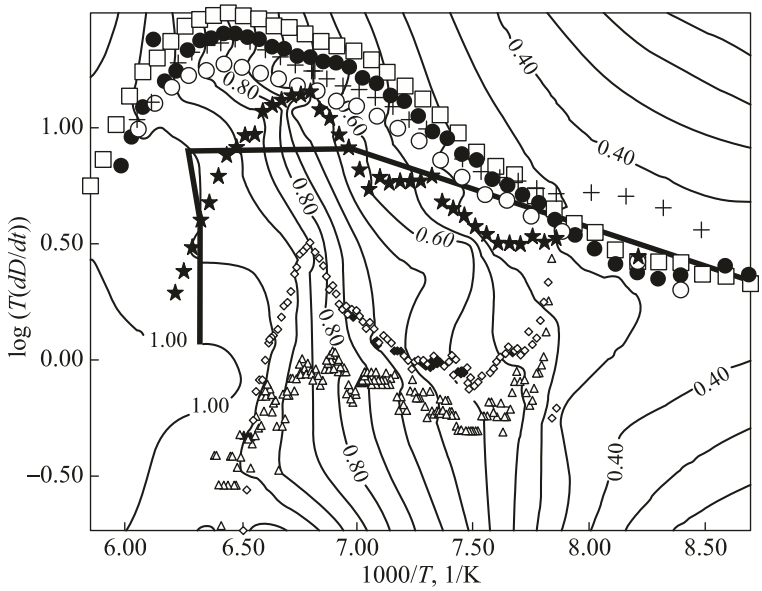

Fig. 3. KFR and modified RCS for TiN nanopowder with 15 nm grain size [17, 18]

RCS of Nanocomposite Powders Based on Refractory Nitrides. Modified RCS modes were successfully used to consolidate nanostructural composites based on refractory nitrides [15, 17]. To produce materials with a volume of 1.5–4 cm^3, a general process of sintering composites in hydrogen and nitrogen was developed based on dilatometric experiments on sintering of TiN–AlN and TiN–Si_3N_4 compositions in vacuum. The compositions studied in [5, 18] are chatacterized in Table 1.

The following powders were studied: TiN nanopowder (15 nm) produced by PVD method (HC Starck, Germany), AlN nanopowder (20–50 nm) and β-Si_3N_4 nanopowder (30–50 nm) produced by plasma-chemical synthesis (PCT Ltd., Latvia).

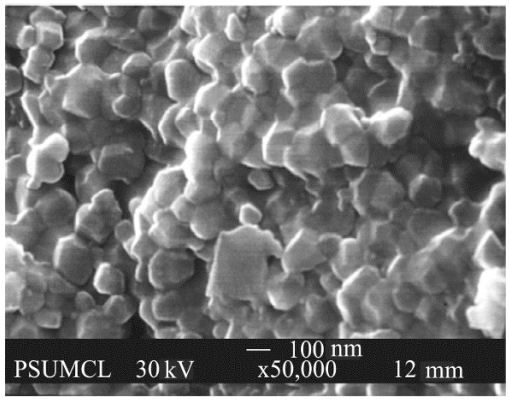

a

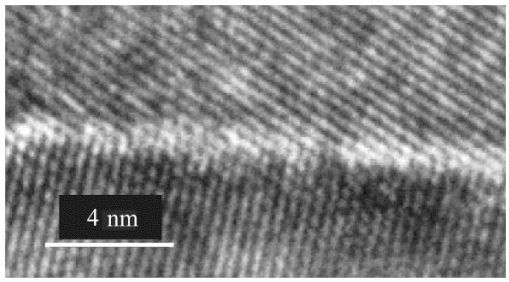

b

Fig. 4. Microstructures (TEM) of RCS consolidated nano-TiN: grained structure (*a*); grain boundaries (*b*)

TABLE 1. Characteristics of TiN-Based Composites, Consolidated in Various Heating Modes

Composite, weight %	Mode	Process parameters		Grain size, nm	Porosity, % (±0.2)
		Atmosphere	T, °C		
TiN–50 Si_3N_4	RCS	Hydrogen	1550	<100	0.6
TiN–50 Si_3N_4	RCS	Nitrogen	1630	>100	0.8
TiN–50 Si_3N_4	CS	Hydrogen	1700	500–1000	0.6
TiN–5 Si_3N_4	RCS	Hydrogen	1650	<100	0.9
TiN–5 Si_3N_4	CS	Hydrogen	1720	500–1000	0.7
TiN–5 AlN	RCS	Vacuum	1600	<100	1
TiN–5 AlN	CS	Vacuum	1700	~ 500	1

The RCS of TiN-based composites was designed using the above-mentioned method [15]. Since the liquid phase may form during sintering of (TiN–Si_3N_4)–6 wt.% Y_2O_3–4 wt.% Al_2O_3 composites, the consolidation mode was adjusted as follows: the RCS runs until the composite density is 85–90% of the theoretical density followed by temperature decrease by 100–150°C and isothermal holding until the total densification of the material. According to the study, the liquid-phase sintering of nanocomposite materials using the RCS mode involving reduction in the temperature at the final stage and isothermal holding for 10–30 min allows obtaining fine-grained ceramics with porosity <1%. For example, by sintering Si_3N_4–TiN composite in hydrogen, it is possible to produce dense nanograined ceramics with porosity less than 1% even at 1550°C, whereas the sintering in nitrogen until the total densification of the composite requires higher temperatures [5]. This effect is associated with the activation of the powder surface in hydrogen and, accordingly, the passivation of the powder surface in nitrogen [17].

Using RCS modes for the consolidation of TiN–AlN composite, a dense, fine-grained ceramics can be obtained even at 1600°C without sintering activators.

A comparison of composites consolidated by modified RCS and conventional sintering (CS) with a constant heating rate and holding would once again point out the advantages of the RCS technology. The sintering was carried out until the composite density reached ~99% of the theoretical density (Table 1). The application of CS for consolidating nanocomposite powders of refractory compounds requires higher sintering temperatures to achieve ~1% porosity, which leads to uncontrolled growth of grains and, therefore, nanograined structure cannot form in the composite.

Figure 5 shows the structure of RCS sintered composites. Their grain size does not exceed 100 nm. In addition, RCS-nanocomposites are characterized by homogeneous grain patterns and porous structure throughout the volume of the product, which guarantees stable properties and is another advantage of the RCS technology.

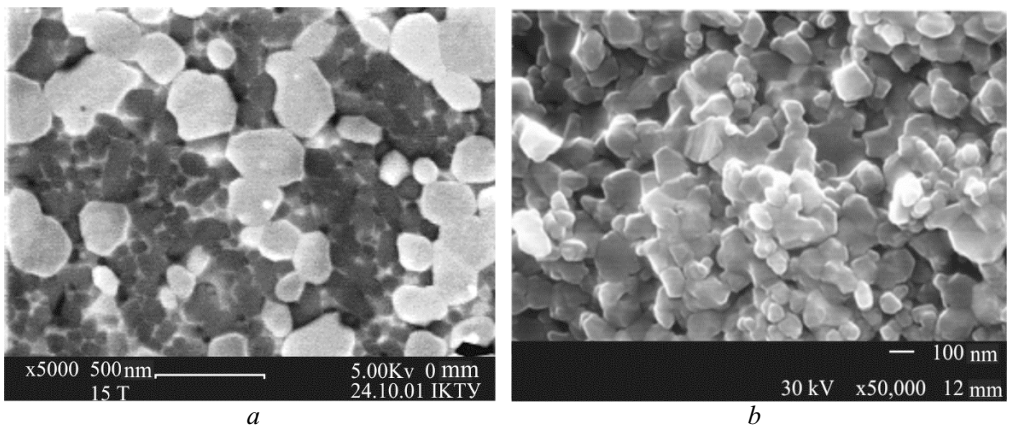

a *b*

Fig. 5. Microstructure (SEM) of sintered composites 50 wt.% TiN–50 wt.% Si_3N_4 (*a*) and TiN–5 wt.% AlN (*b*)

SPS OF NANOCERAMICS BASED ON REFRACTORY COMPOUNDS

The electric-discharge sintering (EDS) is another modern sintering technology that provides much quicker densification and is also successfully used for the consolidation of nanoceramics. The EDS is a hot pressing technique where the current is passed through a heated powder-filled die mold. The recent interest in EDS is associated with new equipment made by FCT Systems (Germany) and Sumitomo (Japan). This equipment allows automation of the consolidation process, obtaining of products with a diameter of more than 300 mm, and a high heating rate (~200°C/min) and a pressure of 50–500 MPa. The EDS is also referred to as spark plasma sintering (SPS) or field assisted sintering technique (FAST) [19–23].

SPS is traditionally organized as follows: fast heating at a rate of 100–200°C/min at a pressure of 100–200 MPa followed by holding for several minutes at high temperatures. Using such a mode to consolidate various ceramics allows achieving a density of 95–97% at temperatures 150–300°C lower than during hot pressing or pressureless sintering. In such conditions, however, grains grow rapidly even if the initial nanopowder (30–70 nm) is used, SPS often results in "coarsening" of the structure up to 250–400 nm [19–21].

A new approach to the SPS consolidation of nanopowders of refractory compounds is offered in [22]. Controlling the shrinkage rate in SPS [9, 15] made it possible to develop and test a multistage (nonlinear) sintering process for nanopowders of refractory compounds (Fig. 6). Formally, SPS and hot pressing are comparable processes, whose kinetics can simply be described by the following equation [24]:

$$\frac{1}{D}\frac{dD}{dt} = \frac{B\phi\mu_{\text{eff}}b}{kT}\left(\frac{b}{d}\right)^p\left(\frac{\sigma_{\text{eff}}}{\mu_{\text{eff}}}\right)^n, \tag{3}$$

where D is the relative density; t is time; B is a constant; ϕ is the diffusion coefficient; μ_{eff} is the shear modulus; b is the Burgers vector; d is the grain size; σ_{eff} is the effective pressure applied to the powder material; p and n are exponents depending on the grain size and pressure, respectively [24].

Equation (3) declares that the densification rate is a function of pressure and temperature. In this case, the formation of material structure can be managed by controlling the densification rate through the variation of process parameters such as heating rate and pressure [22].

Nonlinear SPS involves several stages where the pressure (P) and heating rate (V) vary depending on the shrinkage rate. The process proposed in [22, 23] consists of the following stages: first stage with a high heating rate (V_1) lasting until reaching a density of 75%; intermediate stage with reduced heating rate ($V_2 < V_1$); final stage with minimum allowed heating rate ($V_3 < V_2 < V_1$). Relatively low pressure (P_1) (sufficient to ensure good electrical contact) is applied to the powder material at the beginning of the process. During consolidation, the pressure steadily (smoothly) increases and is controlled at the points of changing the heating rate, which allows maintaining high densification rate and achieving high density of the sintered material.

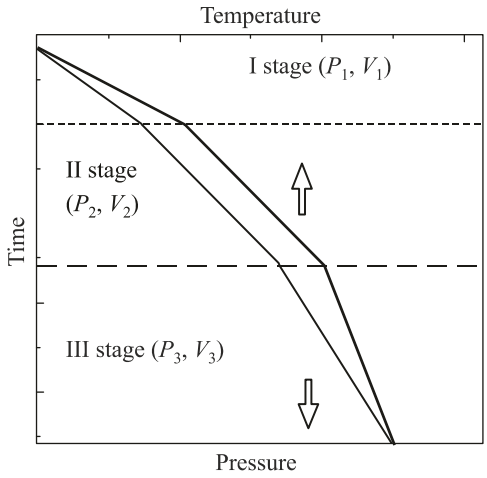

Fig. 6. Nonlinear RCS [23]

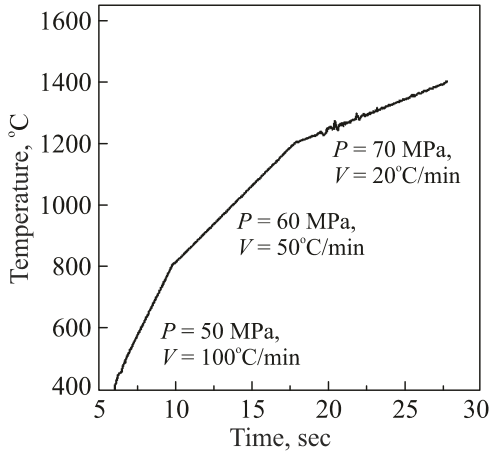

Fig. 7. SPS modes for consolidation of TiCN nanopowders [22]

TABLE 2. Nanopowders and Nanocomposite Mixtures

Nanopowder/Nanocomposite mixture	Maker	d_{av}*, nm	Specific surface, m^2/g	O, wt.%
TiN	HC Stark	17	33	<1.5
TiN–20 wt.% TiB_2	PCT Ltd.	54	26	0.8
$TiC_{0.5}N_{0.5}$	PCT Ltd.	58	56	1.2
Si_3N_4 (nanofibers)	Nanoamor, USA	l = 300–1000 d = 30–100	–	0.9

* Average particle size as per laser granulometry and transmission electron microscopy (TEM).

The densification of the material is mainly stimulated by the rearrangement of particles in the early stages and is a diffusion-controlled process in the final stages. The pressure increase and simultaneous reduction of heating rate in nonlinear SPS prolong the rearrangement of particles (when grain growth is minimal), which makes it possible to form a homogeneous fine-grained structure of the material. At the same time, reducing the heating rate at the final stage allows avoiding holding at high temperatures and obtaining a nanomaterial with density close to the theoretical density.

A nonlinear mode was applied in [22] to consolidate titanium carbonitride nanopowder (70 nm, PCT Ltd.). The application of nonlinear SPS allows reaching 99% of theoretical density at 1400°C and forming fine-grained structure (~100–150 nm), while in the conventional SPS (P = 50 MPa, V = 200°C/min) a density of 97% is achieved only at 1600°C (Fig. 7).

SPS Consolidation of Refractory Nanocomposites. Nonlinear SPS can successfully be applied to consolidate refractory nanocomposites. For example, nonlinear SPS was used in [23] to consolidate composites based on nanopowders of titanium nitride, titanium diboride, silicon nitride, and titanium carbonitride. Table 2 summarizes the characteristics of nanopowders and nanocomposite mixtures.

The experiments were performed on 25 HPD commercial equipment (FCT Systems, T_{max} = 2400°C, P_{max} = 250 kN), using graphite die molds with a diameter of 30 and 70 mm. Nanocomposites TiN (hardened with nanofibers Si_3N_4), Si_3N_4 (nanoparticles–nanofibers with Y_2O_3 and Al_2O_3 additives), TiCN–50 wt.% Si_3N_4, and TiN–20 wt.% TiB_2 were sintered using nonlinear SPS in the pressure range 50–100 MPa and heating rate range 100–20°C/min without isothermal holding at high temperatures.

The nonlinear sintering mode can be successfully used to produce nanocomposites based on materials with different types of conductivity. The composites sintered in nonlinear modes [23] demonstrated structure with a

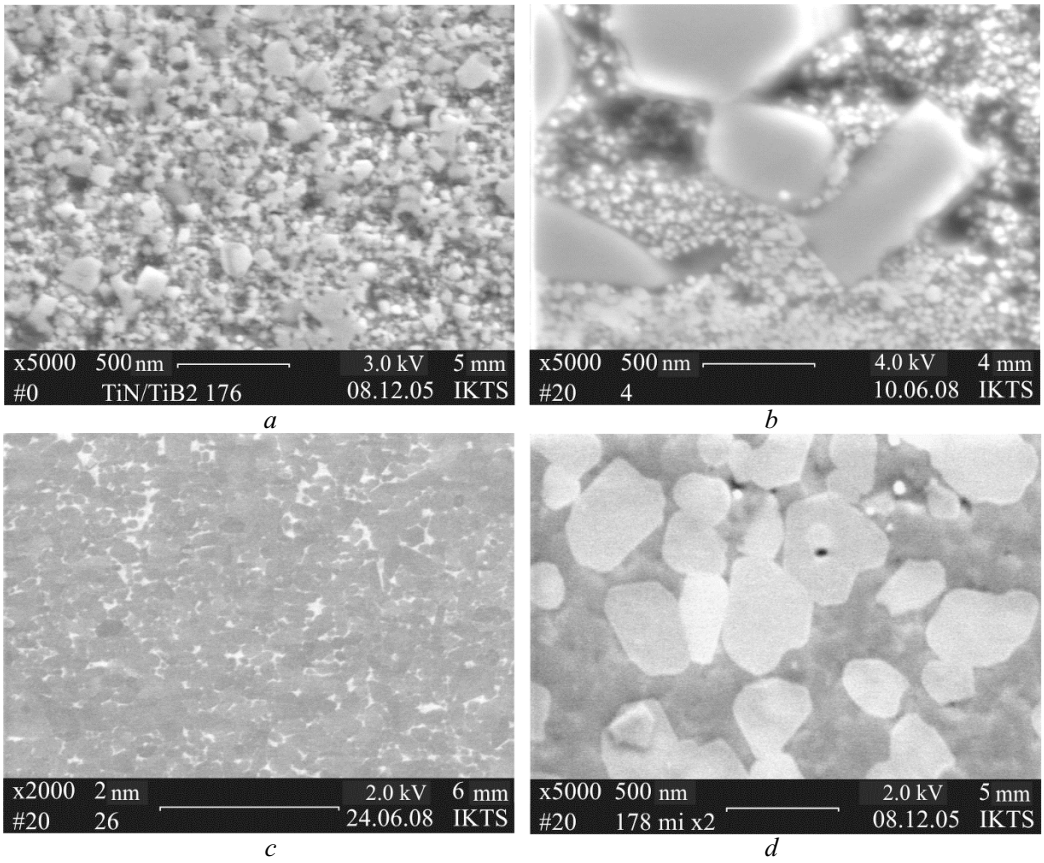

Fig. 8. Microscopy (SEM) of SPS composites: TiN–20 wt.% TiB_2 (*a*); TiN, reinforced with Si_3N_4 nanofibers (*b*); Si_3N_4 nanoparticles–nanofibers (*c*); TiCN–50 wt.% Si_3N_4 (*d*)

grain size of 100–150 nm (Fig. 8) and residual porosity less than 2%. The composite TiN–20 wt.% TiB_2, consisting of phases with high electrical conductivity was consolidated in nonlinear mode into a dense homogeneous nanoceramics (average grain size less than 100 nm) at 1470°C (Fig. 8*a*). In addition, the nanocomposites TiN (reinforced with nanofibers Si_3N_4) and TiCN–Si_3N_4 (with a high content of electrically conductive phase) were successfully sintered to a porosity less than 2% without using special additives (Y_2O_3, Al_2O_3, MgO, etc.) for promoting shrinkage (Figs. 8*c* and 8*d*).

The application of nonlinear SPS to produce nanofiber-reinforced ceramics based on silicon nitride helped to form a nanograined structure without changing the phase composition (Fig. 8*b*).

Lower sintering temperature in nonlinear SPS modes and the possibility to consolidate refractory composites without special additives are a good stimulus for further research on producing nanocomposites with a grain size of 10–20 nm and, consequently, significant improvement in the properties of these materials.

NANOCOMPOSITES PRODUCED BY RCS AND SPS TECHNIQUES: APPLICATION AND PROPERTIES

Nanocomposites based on refractory compounds are traditionally used as cutting tools in the finishing of materials and as wear-resistant products for a wide variety of applications [5, 24–26]. The main advantage of the RCS and SPS technologies for refractory nanocomposites is easy adaptation to commercial equipment and high reproducibility of results.

Figure 9 demonstrates the experimental lots of ceramic cutting plates and RCS ceramic bearing parts based on refractory nitrides produced by the Frantsevich Institute for Problems of Materials Science (FIPMS), NAS of Ukraine.

a

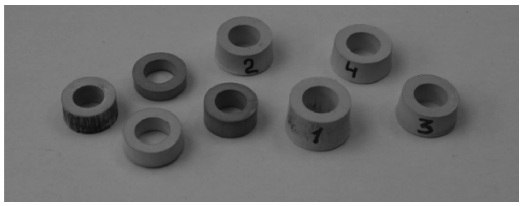

b

Fig. 9. RCS products: cutting plates, based on TiN–Si_3N_4 nanocomposite (*a*); bushes for ceramic bearings, based on Si_3N_4 reinforced with nanofibers (*b*)

A comparative analysis of the properties of the nanocomposites (made from the same initial powders, but by different techniques) was carried out to illustrate the benefits of the RCS and SPS techniques, traditionally used for sintering of refractory composites. The results of mechanical and tribological tests are presented in Table 3. The Vickers hardness and fracture toughness of sintered composites were measured using 100 g and 2 kg loads, respectively, on an MMT-3 tester (Buehler, Germany). The total porosity was determined as per GOST 2409–95 (ISO 5017–88).

TABLE 3. Properties of Refractory Composites

Composite, wt.%	Consolidation mode	Process parameters*	Porosity, %	*d*, nm	Hardness, GPa	Fracture toughness, MPa · $m^{1/2}$	f_{fr}
Si_3N_4–50TiN (Y_2O_3, Al_2O_3)	Modified RCS	1450°C	0.5	50–70	20.5 ± 0.9	6.3	0.38
Si_3N_4–50TiN (Y_2O_3, Al_2O_3)	CS	1650°C	0.7	>500	19.8 ± 1.2	–	0.78
TiCN–50Si_3N_4 (Y_2O_3, Al_2O_3)	CS	1700°C	1.8	>500	17.5 ± 0.6	6	–
TiN–20TiB_2	Nonlinear SPS	1470°C, 50–70 MPa, 20–100 K/min	1.3	<100	22.5 ± 2.1	4.1	–
TiN–20Si_3N_4	Nonlinear SPS	1300°C, 50–70 MPa, 20–100 K/min	1.9	<100	20.3 ± 1.8	5.3	0.42
TiCN–50Si_3N_4	Nonlinear SPS	1450°C, 50–70 MPa, 20–100 K/min	1.2	<100	19.6 ± 1.6	5	0.45
TiCN–50Si_3N_4	SPS	1600°C, 80 MPa, 200 K/min	4	300–500	16 ± 0.6	4.8	0.67

* Temperature *T* (°C), pressure *P* (MPa), and heating rate *V* (K/min).

The wear-resistance of ceramics was tested with an M-22M friction tester (FIPMS, Ukraine) in dry friction between ceramic surface (sample) and VK6 hardmetal shaft (counterface) under a load of 10 kg. The coefficient of friction f_{fr} in this case was determined by the formula:

$$f_{fr} = \frac{F_{fr}}{F}\cos 45^{\circ}, \tag{4}$$

where F_{fr} is the friction force; F is the external load; 45° is half the angle between the surface and the counterface.

Materials consolidated by modified RCS and nonlinear SPS demonstrated a moderate increase in the mechanical characetristics in comparison with composites produced by conventional linear modes of heating. For example, nonlinear SPS helped to produce a dense nanograined ceramics (Fig. 8*d*) TiCN–Si_3N_4, with a sintering temperature 150°C lower than in conventional SPS and, thereby, substantially improved their mechanical and tribotechnical properties. The RCS technique is also characterized by lower sintering temperature, which allows creating a homogeneous nanostructure and, consequently, improving the properties of the material. A comparative study of the properties of ceramics consolidated by the rate-controlled shrinkage technique and ceramics produced by the conventional technology showed an increase in hardness by ~15% and fracture toughness by ~5%. However, the best results were obtained in wear-resistance tests on nanoceramics (Table 3). The coefficient of dry friction for TiCN(TiN)–Si_3N_4 nanocomposites decreased by 40–50% compared with a similar material with submicron structure.

The effect of decrease the friction coefficient and the wear rate of a material and increase in its service life (in 1.5–2 times for TiN–Si_3N_4 nanoceramics) in conditions of dry friction or incomplete lubrication is also described in [25]. On the basis of a comparative analysis of silicon nitride composites obtained by SPS and hot pressing, SPS is demonstrated in [26] to be a very promising technique to obtain dense nanostructured materials for tribotechnical purposes.

The highly improved properties of SPS- and RCS-consolidated nanoceramics based on refractory compounds opens up new prospects for the implementation of nanocomposites in aerospace engineering, power engineering, materials processing, medical technology, and biotechnology.

However, the consolidation methods contemplated herein have their weaknesses. The main disadvantage of RCS and nonlinear SPS is that they are not universal. The RCS and SPS techniques designed for the consolidation of nanopowders or nanocomposite mixtures of one particle size cannot be directly applied to the sintering of the same materials with different size of powder particles. This means that if one changes the raw material (nanopowder) supplier, then it will be necessary to conduct primary studies and to design the RCS-profile or to select a mode (as in nonlinear SPS).

It should be noted that, despite the large number of theoretical and applied studies on the consolidation of nanomaterials, there is yet no hypothesis on the structure–properties relationship for nanomaterials. The same nanomaterials with the same size of structural elements, but produced by different methods show significantly different values of the measurable characteristics. This is primarily due to the differences in the formation of grain boundaries in nanomaterials produced by different methods.

The importance of grain boundaries in the formation of nanomaterial properties is demonstrated by the increasing number of thorough studies related to grain boundary engineering intended to achieve the best possible material properties [27, 28].

CONCLUSIONS

New approaches to the consolidation of nanoceramics based on control of densification rate in combination with modern equipment definitely allow manufacturing products based on refractory compounds with grain size less than 100 nm.

The SPS and RCS consolidation techniques are used to demonstrate the benefit of using nonlinear modes of sintering refractory nanopowders to obtain dense nanostructural ceramics.

The RCS method can be successfully applied to the consolidation of composites based on silicon nitride in liquid-phase sintering and composites of titanium and aluminium nitrides. RCS composites based on refractory nitrides are characterized by homogeneous grain and porous structure throughout the volume of the product, which guarantees the stability of the composite properties.

It is expedient to apply nonlinear SPS modes to composites with high content of conductive phase (TiN–TiB_2, TiCN (TiN)–Si_3N_4). Using such SPS mode makes possible to achieve the ultimate density of ceramics of 95–97% of the theoretical density at temperatures 150–300°C lower than during hot pressing or pressureless sintering, as well as to form a homogeneous nanostructure.

Noteworthy is the significant increase of the mechanical (5–15%) and tribotechnical (up to 50%) properties of the nanocomposites consolidated by RCS, modified SPS, and nonlinear SPS.

A comparison of the properties of nanostructured composites and submicron ceramics has shown that the friction coefficient for composite nanomaterials based on refractory compounds is lower by a factor of 2. This effect is regarded as promising for creating a new generation of wear-resistant nanomaterials based on refractory compounds for use in dry friction conditions at high temperatures.

ACKNOWLEDGEMENTS

The author thanks M. Herrmann and Ya. Rotel (IKTS, Germany) for assistance in SPS experiments, V. T. Varchenko (FIPMS, Ukraine) for assistance in experiments on ceramics wear-resistance, and A. V. Ragulya (FIPMS, Ukraine).

REFERENCES

1. D. A. Konstantinidis and E. C. Aifantis, “On the anomalous hardness of nanocrystalline materials,” *Nanostruct. Mat*., Vol. 7, No. 10, 1111–1118 (1998).
2. R. A. Andrievsky, “State of the art and perspectives in the field of particulate nanostructured materials (Review),” *J. Mater. Sci. Technol*., **14**, 97–103 (1998).
3. S. Veprek and P. Nesladek, “Superhard nanocrystalline composites with hardness of diamond,” *Phys. St. Sol*., No. 177, 53–62 (1999).
4. V. G. Gryaznov, I. A. Polonsky, A. E. Romanov, and L. I. Trusov, “Size effect of dislocation stability in nanocrystals,” *Phys. Rev. B*., **44**, 42–46 (1991).
5. O. B. Zgalat-Lozynskii, A. V. Ragulya, and M. Herrmann, “Nanostructured composites based on high-melting nitrides,” *Silicates Industries*, **69**, No. 7–8, 147–152 (2004).
6. D. T. Castro and J. Y. Ying, “Synthesisand sintering of nanocrystalline titanium nitride,” *Nanostruct. Mat*., **9**, 67–70 (1997).
7. T. Rabe and R. Wasche, “Sintering behavior of nanocrystalline titanium nitride powders,” *Nanostruct. Mat*., **6**, No. 3, 357–360 (1995).
8. III H. Palmour and D. R. Johnson, “Phenomenological model for rate-controlled sintering,” in: *Sintering and Related Phenomena*, Gordon & Breach Publishers, New York (1967), p.779.
9. A. V. Ragulya, “Rate-controlled synthesis and sintering of nanocrystalline barium titanate powder,” *Nanostruct. Mat*., **10**, No. 3, 349–355 (1998).
10. A. I. Bykov, A. V. Polotai, A. V. Ragulya, and V. V. Skorokhod, “Synthesis and sintering of nanocrystalline barium titanate powder under nonisothermal conditions. Part V. Nonisothermal sintering of barium titanate powders of different dispersion,” *Powder Metall. Met. Ceram*., **39**, No. 7/8, 395–402 (2000).
11. V. V. Skorokhod and A. V. Ragulya, “Sintering at a controlled rate as a method for regulating the microstructure of ceramics and similar sintered materials,” *Powder Metall. Met. Ceram*., **33**, No. 3/4, 109–117 (1994).
12. A. V. Ragulya and V. V. Skorokhod, “Validity of the rate-controlled sintering method for consolidation of dense nanocrystalline materials,” in: *Proc. 14th Plansee Seminar*, Vol. 2, Plansee AG (1997), pp. 735–744 .

13. V. V. Skorokhod and A. V. Ragulya, “Evolution of the porous structure during non-isothermal sintering of fine powders,” *Sci. Sintering*, **27**, 89–98 (1995).
14. A. V. Ragulya and V. V. Skorokhod, “Rate-controlled sintering of ultrafine nickel powder,” *Nanostruct. Mat*., **5**, No. 7, 835–844 (1995).
15. O. B. Zgalat-Lozynskii, V. V. Skorokhod, A. V. Ragulya, et al., “Sintering of refractory compound nanocrystalline powders. Part 2. Non-isothermal sintering of titanium nitride powder,” *Powder Metall. Met. Ceram*., **40**, No. 11–12, 537–581 (2001).
16. I.-Wei Chen and X.-H. Wang, “Sintering dense nanocrystalline ceramics without final-stage grain growth,” *Nature*, **404**, 168–171 (2000).
17. O. B. Zgalat-Lozynskii, A. V. Ragulya, and M. Herrmann, “Rate-controlled sintering of nanostructured titanium nitride powders,” *Series II: Mathematics, Physics and Chemistry*, **16**, 161–167 (2000).
18. O. B. Zgalat-Lozynskii, A. V. Ragulya, and M. Herrmann, “TiN-based nanocrystalline ceramics,” *Key Eng. Mat*., 206–213, 2181–2184 (2001).
19. J. R. Groza, J. D. Curtis, and M. Kramer, “Field-assisted sintering of nanocrystalline titanium nitride,” *J. Am. Ceram. Soc*., **83**, No. 5, 1281–1283 (2000).
20. M. Nygren and Z. Shen, “On the preparation of bio-, nano- and structural ceramics and composites by spark plasma sintering,” *Sol. St. Sci*., **5**, 125–131 (2003).
21. P. Angerer, L. G. Yu, K. A. Khor, et al., “Spark-plasma-sintering (SPS) of nanostructured titanium carbonitride powders,” *J. Europ. Ceram. Soc*., **25**, No. 11, 1919–1927 (2005).
22. O. B. Zgalat-Lozynskii, M. Herrmann, and A. V. Ragulya, “Spark plasma sintering of TiCN nanopowders in non-linear heating and loading regimes,” *J. Europ. Ceram. Soc*., Vol. 31, 809–813 (2011).
23. O. B. Zgalat-Lozynskii, A. V. Ragulya, M. Herrmann, et al., “Structure and mechanical properties of spark plasma sintered tin-based nanocomposites,” *Archives Metal. Mat*., **57**, No. 3, 853–858 (2012).
24. G. Bernard-Granger and C. Guizard, “Spark plasma sintering of a commercially available granulated zirconia powder: I. Sintering path and hypotheses about the mechanism(s) controlling densification,” *Acta Mat*., **55**, 3493–3504 (2007).
25. M. Schulz, I. Herrmann, I. Endler, et al., “Nano Si_3N_4 composites with improved tribological properties,” *Lubrication Sci*., **21**, 69–81 (2009).
26. M. Herrmann, Z. Shen, I. Schulz, et al., “Silicon nitride nanoceramics densified by dynamic grain sliding,” *J. Mater. Res*., **25**, No. 12, 2354–2361 (2010).
27. S. Gregory, “Rohrer measuring and interpreting the structure of grain-boundary networks,” *J. Am. Ceram. Soc.*, **94**, No. 3, 633–646 (2011).
28. A. M. Glezer, N. A. Shurygina, E. N. Blinova, at al., “Grain boundary engineering as a way to achieve the ultimate (theoretical) strength of nanocrystals,” *Deform. i Razrush. Mater*., No. 11, 1–7 (2011).